Mechanics & Industry **17**, 504 (2016)

DOI: 10.1051/meca/2015108
www.mechanics-industry.org

Mechanics & Industry

Antibacterial activity of monolayer nanoparticulate Ag_N-(titanium-oxo-alkoxy) coatings

Zixian Jia[1], Viktor Nadtochenko[2,3,4], Marina A. Radzig[5], Inessa A. Khmel[5], Gennadii Zavilgelsky[6], Rabah Azouani[7,a], Christine Mielcarek[7], Mounir Ben Amar[1], Mamadou Traore[1] and Andrei Kanaev[1]

[1] Laboratoire des Sciences des Procédés et des Matériaux, CNRS, Université Paris 13, Sorbonne Paris Cité, 93430 Villetaneuse, France
[2] N. N. Semenov Institute of Chemical Physics, RAS, 119071 Moscow, Russia
[3] Institute of Problem of Chemical Physics, RAS, 142432 Chernogolovka, Russia
[4] Moscow Institute of Physics and Technology, 141700 Dolgoprudny, Moscow Region
[5] Institute of Molecular Genetics, RAS, 123182 Moscow, Russia
[6] State Research Institute of Genetics and Selection of Industrial Microorganisms, 117545 Moscow, Russia
[7] École de Biologie Industrielle (EBI), 13 boulevard de l'HAUTIL, 95092 Cergy Pontoise, France

Received 8 April 2015, Accepted 14 November 2015

Abstract – A comparative evaluation of the antibacterial effect of silver in the form of nanoparticles and Ag^+ ions was performed. Silver nanoparticulate coatings of stable and reproducible morphology were prepared on monolayer size-selected titanium-oxo-alkoxy nanoparticles deposited on glass substrates. The coatings exhibit a strong antibacterial activity towards *Escherichia coli* K12 AB 1157 and suppress biofilms formation. This activity is mainly related to the Ag^+ ions release into aqueous solutions in dark. The deposited silver mass ~1 $\mu g.cm^{-2}$ is smaller compared to that of Ag^+ ions and nanoparticles generally reported for inhibiting *Escherichia coli*. The synergetic effect of the deposited nanoparticles and Ag^+ ions can be suggested.

Key words: Ag-TiO_2 / nanoparticles / nanocoatings / antibacterial activity

1 Introduction

Silver-based compounds are used as disinfection agents since a long time. A reason is that silver ions are highly toxic to microorganisms showing strong biocide effects [1–3]. Recently, silver in the form of nanoparticles (AgNP) was recognized to possess even more powerful action against bacteria, including multiresistant to antibiotics bacterial strains, against viruses and fungi. Although the mechanisms of the silver cation action on bacterial cells have been studied over long time, they remain only partially understood; those of the AgNP action are even not yet clear. Silver ions were shown to interact with nucleic acids and associate mainly with bases in DNA rather than with phosphate groups; it is assumed that in these conditions the DNA cell loses its ability to replication [4]. A reported similarity in actions of silver ions and AgNP on cells suggests that a significant ions release takes place in AgNP; this mechanism is considered as the most relevant and even dominant in explanation of the antimicrobial effect. As a source of the ions, silver coatings morphology appears to be an important factor of the bacteria suppression activity.

Despite of the ions effect, the direct action of AgNP as antimicrobial agent cannot be excluded [5–7]. In fact, the penetration of AgNP the cell membrane and intracellular accumulation has been evidenced by electron microscopy [8,9]. AgNP were suggested to have a pleiotropic action on bacterial cells. They are attached to the cell membrane and disturb its permeability, which results in its destabilization and sharp decrease of the potential, exhaustion of intracellular ATP and inhibition of the cell respiration. AgNP or released cations can bind to thiol groups of different proteins perturbing their activity. All this can result in the cell death [9–13]. It is however difficult to distinguish the effect of AgNP and released Ag^+ ions. To date, the biological impact of silver nanoparticles and ions is still under debates [14].

Apart for the action on a single bacterium, a complementary verification of the AgNP activity against biofilms is required. In fact, more than 99% bacteria survive in

[a] Corresponding author: r.azouani@hubebi.com

form of biofilms with a characteristic architecture enclosed in exopolymer matrix, attached to surfaces. In such environment, pathogenic bacteria possess a much higher resistance to antibiotics and other antibacterial drugs, which creates great difficulties of their elimination in medical practice [15]. The formation of biofilms on implanted devices (e.g., catheters, lenses, artificial heart valves, etc.) leads to the development of chronic diseases. In this connection, special attention should be paid to studies of the AgNP effect on the biofilm formation. It has been recently demonstrated that silver nanoparticles of 8.3 nm size stabilized by casein peptides sharply inhibited biofilm formation of *Escherichia coli* AB1157, *Pseudomonas aeruginosa* PAO1 and *Serratia proteamaculans* 94 in concentrations 5 μg.ml^{-1}, 10 μg.ml^{-1} and 10 μg.ml^{-1}, respectively [16]. The viability of *E. coli* AB1157 cells in developed biofilms decreased considerably at AgNP concentrations higher than 100−150 μg.ml^{-1}. *E. coli* strains with mutations in genes responsible for the repair of DNA containing oxidative lesions (*mutY, mutS, mutM*, *mutT, nth*) were less resistant to AgNP than wild-type strain. It suggests that these genes can be involved in the repair of damages in DNA caused by AgNP. *E. coli* mutants deficient in excision repair, SOS response and in the synthesis of global regulators RpoS, CRP protein and Lon protease did not differ in sensitivity to AgNP from the wild-type cells. LuxI/LuxR Quorum Sensing systems did not participate in the control of sensitivity/resistance to AgNP of *Pseudomonas* and *Serratia* tested strains. It was found that *E. coli* mutant strains deficient in OmpF or OmpC porins were 4−8 times more resistant to AgNP as compared to the wildtype strain. It indicates that porins are important factors of AgNP antibacterial effect.

An interesting strategy to inhibit bacterial survival and colonization is the immobilization of silver species on surfaces. In the present work we study the antibacterial and anti-biofilm activity of Ag-titanium-oxo-alkoxy (TOA) nanoparticulate coatings of highly stable and reproducible morphology. We compare the effect of the deposited AgNP with that of Ag^+ ions. Since the detachment of AgNP and penetration inside the bacterial cell is excluded in our experimental conditions, the antimicrobial effect of AgNP can be clarified.

2 Materials and methods

2.1 Materials

AgNP nanoparticles were grown on monolayer coatings of titanium oxo-alkoxy (TOA) nanoparticles, according to the procedure described by Jia et al. [17]. It consists in coverage of a glass plate of 45×24 mm^2 size by a monolayer of size-selected 5-nm TOA nanoparticles [18] of low roughness (∼0.5 nm) followed by silver ions reduction from aqueous solution of $AgNO_3$ at UV-A lamp (Philips) irradiation in the spectral range of 362 ± 10 nm with the power density of 6.9 mW.cm^{-2}. This procedure results in a stable AgNP morphology of spherical segments with $h/D = 1/4$ and $D = 12$ nm (where h and D are height and diameter of the particles) and the deposited mass of about 200 ng.cm^{-2}, when running the process over sufficiently long time until saturation. The saturation in our preparation conditions begins after 10 min of the deposition process duration. In contrast, in the process beginning ($t < 10$ min), the deposition mass linearly increases with time: both size and particles number density increase at this stage.

The analysis of the dissolved silver is done using iCAP 6000 THERMO device with 0.1 μg.L^{-1} precision. The plate was immersed into 30 ml of distilled deionised water for 1 day in dark conditions, than withdrawn, dried and immersed in next pure 30 ml of water, and so on. Each portion of water was conserved for the subsequent analysis. The measurements are calibrated using 0.02 mol.L^{-1} nitric acid solution.

2.2 Bacterial strain, growth conditions

Bacterial strain used in the work was *Escherichia coli* K12 AB1157. It was maintained on Luria-Bertani broth solid (1.5% of agar) medium (LA, Sigma) at 30 °C. Difco nutrient broth (NB) and Difco nutrient agar (NA) were used according to the protocol described in references [16,19] in experiments with AgNP/TiO_2.

The bacteria cells for MICs measurements were cultured in NB medium. MIC value of $AgNO_3$ for *E. coli* AB1157 measured in the present work is equal to 0.10 ± 0.05 $AgNO_3$ μg.ml^{-1} that is in a good agreement with the previous MIC measurements 0.11 ± 0.05 μg.ml^{-1} [16]. Minimum inhibitory concentrations of (MICs) of $AgNO_3$ were measured by serial twofold dilution [20]. Initial CFU.ml^{-1} was 1×10^5 in NB. The concentration of planktonic cells was evaluated by taking the optical density at 600 nm (OD_{600}). The measurements were made after incubation of bacteria for 24 h at 30 °C.

E. coli cells were grown in NB for a night and then 100-fold diluted in fresh NB. Cultures were incubated at 30 °C with aeration. An overnight culture of the strain was diluted to $\sim 2.5 \times 10^7$ CFU.ml^{-1} in fresh warm NB supplemented. Optical density of cell suspension at 600 nm (OD_{600}) and CFU.ml^{-1} was measured. To determine CFU.ml^{-1} of E. coli, cells were plated on NB solid medium, and the plates were incubated at 30 °C. The number of colonies was counted after 24 h of incubation. Experiments were repeated 5 times and bacteria were grown in 8 replicate wells in each experiment.

The biofilm formation of tested strains was analyzed as described previously [16,21,22]. Cells from fresh LA medium were inoculated into NB and incubated under shaking for 24 h at 30 °C. The cultures were then 300-fold diluted in fresh NB supplemented with $AgNO_3$ or AgNP-TOA samples. Inoculated cultures were grown in 96-well polystyrene microtiter plates (150 μl per well) for 24 h at 30 °C under shaking (105 rpm). The growth of planktonic (unattached) cells was evaluated by the optical density at 600 nm (OD_{600}). Biofilm formation was measured by discarding the medium, rinsing the wells with distilled

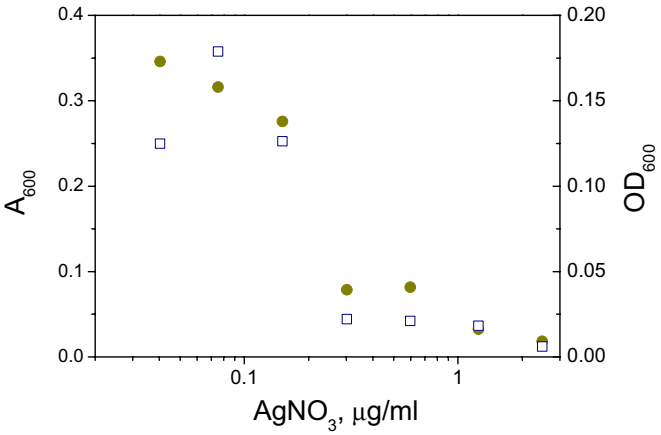

Fig. 1. Effect of $AgNO_3$ on biofilm formation and planctonic cells: optical density (OD_{600}) of planctonic cells (●) and absorption (A_{600}) of crystal violet staining of biofilms (□).

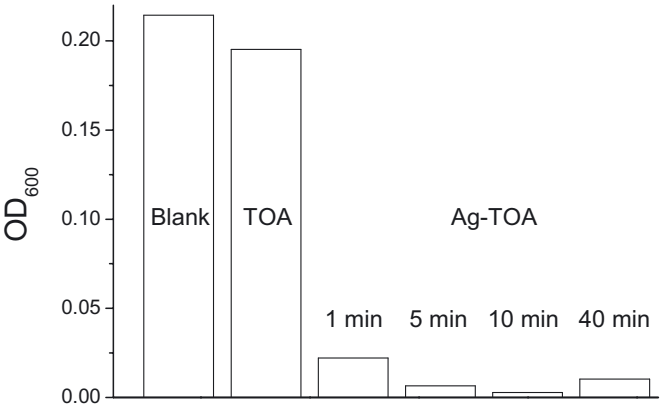

Fig. 2. Optical density at 600 nm (OD_{600}) of the *E. coli* planktonic form after 24 h exposition at 30 °C. The labels indicate supporting glass plate (Blank), pure TOA and composite Ag-TOA nanocoatings prepared by Ag^+ ions reduction during 1, 5, 10 and 40 min.

water, and staining of the attached cells with crystal violet. After staining, the liquid was discarded and the wells rinsed with distilled water three times, then the biofilm-associated crystal violet was solubilized with ethanol, and the absorbance at 600 nm was measured. A microplate reader (Model 2550 Microplate Reader, Bio-Rad, USA) was used for measuring planktonic growth and biofilms. The bacterial growth for 24 h was found to be optimal for biofilm formation. At longer growth times, the level of biofilm formation did not change or even decreased. Experiments were repeated 5 times and bacteria were grown in 8 replicate wells in each experiment.

3 Results and discussion

3.1 Effect of Ag/TOA and $AgNO_3$ on the inactivation of planktonic E. coli and on the formation of biofilms

Figure 1 illustrates the effect of $AgNO_3$ on the planktonic growth and biofilm formation evaluated by the absorbance of crystal violet at A_{600} for bacteria *E. coli* AB1157. The optical density OD_{600} decreases to almost zero at $AgNO_3$ concentrations higher than 0.3 $\mu g.ml^{-1}$ for *E. coli* AB1157. Simultaneous declines of the planktonic growth and biofilm formation with an increase of the $AgNO_3$ concentrations suggest that the same mechanism is responsible for both effects.

Ag/TiO_2 coatings strongly inhibit the biofilm formation until no biofilm was observed. Figure 2 demonstrates the effect of AgNP-covered TiO_2 plates on the planctonic *E. coli* population after incubation under shaking for 24 h at 30 °C. Initial concentration of cells was 10^7 $CFU.ml^{-1}$. The optical density (OD_{600}) related to the bacterial cells decreases almost to the zero level in all prepared AgNP-TOA coatings with different silver deposited masses. According to reference [17], the deposited 12-nm silver nanoparticles cannot be a sufficient

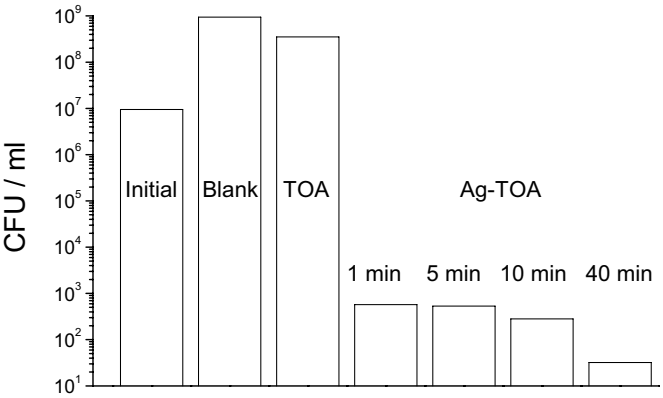

Fig. 3. $CFU.ml^{-1}$ of bacteria on prepared samples after incubation under shaking for 24 h at 30 °C. The Initial column indicates the input $CFU.ml^{-1}$ level. The labels indicate supporting glass plate (Blank), pure TOA and composite Ag-TOA nanocoatings prepared by Ag^+ ions reduction during 1, 5, 10 and 40 min.

source of Ag^+ ions necessary for the bacteria suppression: ∼0.3 $\mu g.ml^{-1}$ in Figure 1. Below we address this point in Chapter devoted to the AgNP film dissolution.

In order to provide more precision to the assay remaining cells, additional experiments with seeding of cells on an agar medium were carried out. Figure 3 depicts that in blank experiment (no TiO_2 no Ag/TiO_2) and in the control experiment (only TiO_2 at the glass plate) a growth of the cells population is detected after incubation. In contrast, in presence of photodeposited AgNP onto TOA-covered glass plates during 1 min and 5 min, the $CFU.ml^{-1}$ level decreases down to about 6×10^2, for 10 min $CFU.ml^{-1}$ is about 3×10^2 and for 40 min it is even lower 40. Accordingly, by increasing the deposited AgNP mass the cells population strongly decreases, but not disappears.

Moreover since the supported AgNP on the monolayer TOA nanoparticle film of our samples cannot penetrate

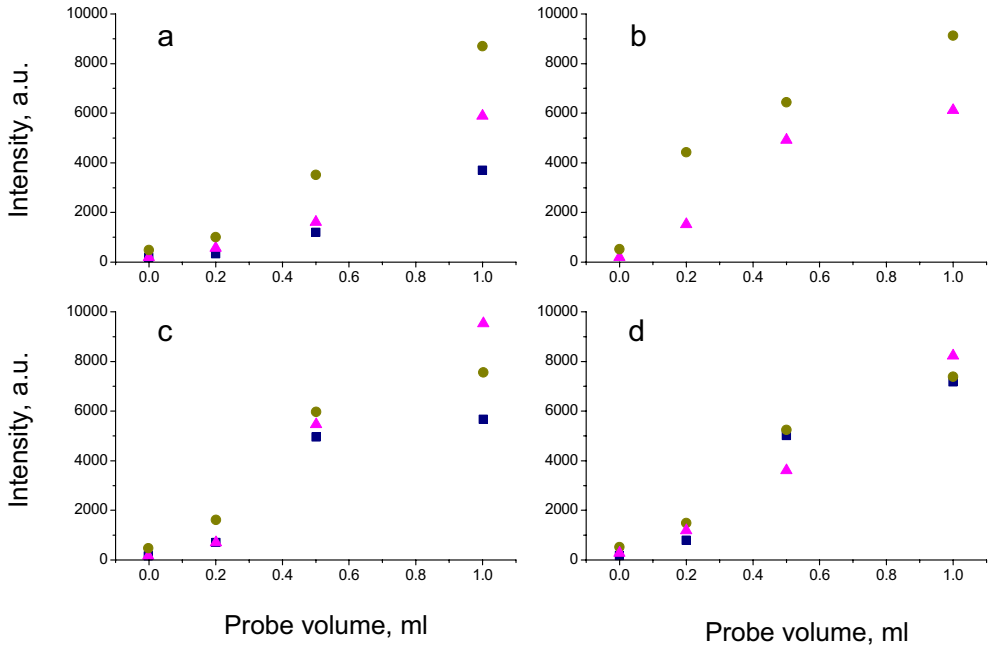

Fig. 4. Bioluminescence intensity of *E. coli* MC1061 (pCopA' ::lux) biosensor as a function of the probe volume in contact with different AgNP films grown for 1 (a), 5 (b), 10 (c) and 40 (d) min. The contact time of biosensor with supernatant is 30 (■), 60 (▲) and 120 (●) min.

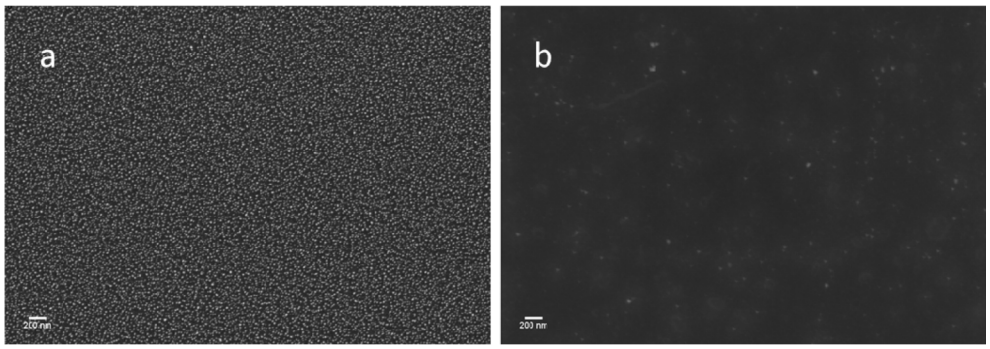

Fig. 5. SEM images of the deposited silver nanoparticles before (a) and after 6 standings in water (b) (each one during 1 day in 30 ml of water) in series 2.

the cells, we conclude about a dominant role of the solvated Ag^+ ions in the observed antibacterial activity.

A formal prove of the presence of solvated silver ions provide further measurements with a bioluminescent sensor. Its function is to trig synthesis of the luciferase after silver binding to proteins, which last along otherwise blocks the synthesis. Bacterial luciferase catalyzes the oxidation of atmospheric oxygen of long-chain aldehyde RCHO and flavin mononucleotide ($FMNH_2$) [23]: $RCHO + FMNH_2 + O_2 = FMN + RCHOO + H_2O + h\upsilon$ ($\lambda_{max} = 490$ nm). This process is accompanied by a strong luminescence in the blue-green spectral range. This method permits an estimation of the silver ions concentrations at the level of 0.05−0.1 $\mu g.ml^{-1}$ ($AgNO_3$ equivalent). These measurements are shown in Figure 4. The presented data indicate no significant change of the activation time of *E. coli* MC1061 (pCopA' ::lux) biosensor [23] during 30, 60 and 120 min. This indicates the total consumption of the solvated silver ions.

3.2 Measurements of AgNP dissolution

The SEM image of the deposited silver particles (spherical segments) is shown in Figure 5a. The analysis of silver dissolution was performed in two series with respective four (series 1) and six (series 2) successive washings with fresh liquid water at room temperature. The results are presented in Table 1.

The silver mass in the series of water solutions decreases with an increase of the number of standings, which evidence the silver deposit dissolution (in dark conditions). This is confirmed by SEM image in Figure 5b. However even after 6 standings, some large silver nanoparticles remain on the surface.

Table 1. Solvated silver concentration after successive washing of AgNP-TOA coating (obtained after 40 min silver deposition) with 30 ml fresh water during 1 day. Reference sample (Ref.) contains 0.02 mol/L nitric acid solution in water.

Series 1		Series 2	
Number of contacts	Concentration μg.L^{-1}	Number of contacts	Concentration μg.L^{-1}
1	286	1	327
2	53.9	2	33.6
3	36.9	4	24.6
4	17.2	6	12.6
Ref.	12.8	Ref.	12.8

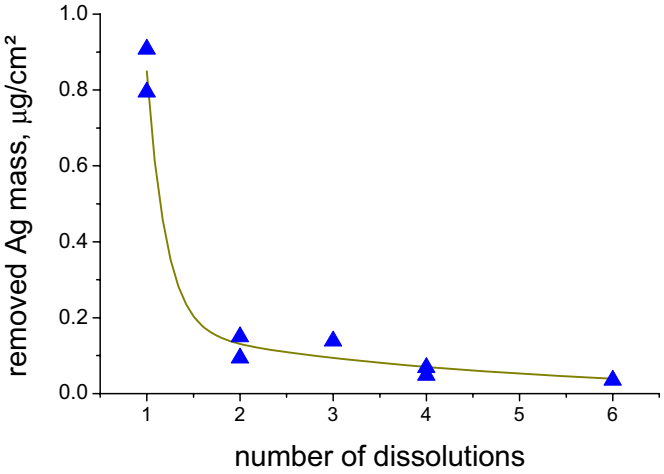

Fig. 6. Silver dissolution curve as a function of a number of standings. The solid line represents the two-exponential fit. The AgNP coating was prepared after the UV-irradiation during 40 min.

The silver dissolution curve is graphically presented in Figure 6. The experimental data can be successfully fitted by two-exponential decay function with time constants 0.2 and 3.5 days, which indicates that the dissolution kinetics involves two sources of silver atoms. These sources are probably atoms and small clusters and limit-size 12-nm nanoparticles.

The total removed mass density in form of silver ions is $\sim$1 μg.cm^{-2}, which is larger compared to that 200 ng.cm^{-2} [17] contained in AgNP observed in SEM images (Fig. 5a). This evidences that a substantial part of the reduced silver (80%) is contained in form of dispersed atoms and small clusters, which size is below the resolution limit of SEM (typically <1 nm). This finding may also explain the saturated nature of the deposition process discussed in reference [17] by the titania surface coverage with silver layer, which slows down the ions reduction rate. Another important consequence of this finding is that the larger nanoparticles possess weaker dissolution ability compared to small clusters and dispersed atoms. This conclusion can find a confirmation in the plate SEM image after 6 silver removal cycles in Figure 5b, which indicates that large AgNP remain.

AgNP are stable in pure water and generally generate Ag^+ ions in presence of solute negative ions, like Cl^- [24]. The mechanism of supported AgNP dissolution in our experiments is not yet clear. However, we tentatively assign this effect to a catalytic action of the monolayer titania nanoparticles, which may transfer silver electron to solvated oxygen molecules.

The total silver concentrations deposited mass in these experiments were 0.3, 1.7, 3.3 and 4 μg for AgNP films grown respectively during 1, 5, 10 and 40 min [17]. In the bacteria inactivation experiments, the films were immersed into a solution of 10 ml volume. Therefore, the total silver concentrations (in form of both nanoparticles and solvated ions) in the solution were below 0.03, 0.17, 0.33 and 0.4 mg.L^{-1} respectively. These values are below those typical of *E. coli* inhibition by Ag^+ ions (0.5 mg.L^{-1}) and AgNP ($\sim$10 mg.L^{-1}) [25] and fit the low-level critical concentrations towards unicellular organisms suppression.

4 Conclusions

We report on fabrication of silver nanoparticulate coatings of stable and reproducible morphology and low deposited mass $\sim$1 μg.cm^{-2} onto monolayer coatings of size-selected (5 nm) titanium-oxo-alkoxy (TOA) nanoparticles deposited on glass substrates. The prepared coatings exhibit a strong antibacterial activity towards *E. coli* K12 AB 1157 and entirely suppress biofilms formation. This activity is related to the Ag^+ ions release into aqueous solutions. The release kinetics is bimodal and suggests a higher solubility of the deposited dispersed atoms and small clusters. The deposited silver mass (in form of nanoparticles, clusters and dispersed atoms) is smaller compared to that of Ag^+ ions and Ag nanoparticles generally reported for inhibiting *E. coli*. The synergistic effect of deposited AgNP and released Ag^+ ions can be suggested. The TOA nanocoating can serve a barrier layer preventing Ag^+/Na^+ exchange with substrates that decreases the AgNP film activity. The applications of AgNP-TOA nanocoatings in a humid environment can be considered.

Acknowledgements. The ANR (*Agence Nationale de la Recherche*) and CGI (*Commissariat à l'Investissement d'Avenir*) are gratefully acknowledged for their financial support of this work through labex SEAM (Science and Engineering for Advanced Materials and devices) ANR 11 LABX 086, ANR 11 IDEX 05 02".

References

[1] R.M. Slawson, M.I. Van Dyke, H. Lee, J.T. Trevors, Plasmid. 27 (1992) 72

[2] G. Zhao, S.E. Stevens, Biometals 11 (1998) 27

[3] M. Singh, S. Singh, S. Prasad, I.S. Gambhir, J. Nanomater. Biostruct. 3 (2008) 115

[4] Q.L. Feng, J. Wu, G.Q. Chen, F.Z. Cui, T.N. Kim, J.O. Kim, J. Biomed. Mater. Res. 52 (2000) 662

[5] F. Furno, K.S. Morley, B. Wong, B.L. Sharp, P.L. Arnold, S.M. Howdle, R. Bayston, P.D. Brown, P.D. Winship, H.J. Reid, J. Antimicrob. Chemother 54 (2004) 1019

[6] D. Roe, B. Karandikar, N. Bonn-savage, B. Gibbins, J.B. Roullet, J. Antimicrob. Chemother. 61 (2008) 869

[7] N.N. Lubick, Environ. Sci. Technol. 42 (2008) 8617

[8] X.N. Xu, W.J. Brownlow, S.V. Kyriacou, Q. Wan, J.J. Viola, Biochemistry 43 (2004) 10400

[9] J.R. Morones, J.L. Elechiguerra, A. Camacho, K. Holt, J.B. Kouri, J.T. Ramirez, M.J. Yacaman, Nanotechnology 16 (2005) 2346

[10] S.K. Gogoi, P. Gopinath, A. Paul, A. Ramesh, S.S. Ghosh, A. Chattopadhyay, Langmuir 22 (2006) 9322

[11] C.N. Lok, C.M. Ho, R. Chen, Q.Y. He, W.Y. Yu, H. Sun, P.K. Tam, J.F. Chiu, C.M. Che, J. Proteome Res. 5 (2006) 916

[12] S. Pal, Y.K. Tak, J.M. Song, Appl. Environ. Microbiol. 73 (2007) 1712

[13] V.A. Nadtochenko, M.A. Radzig, I.A. Khmel, Nanotechnologies in Russia 5 (2010) 277

[14] R. Behra, L. Sigg, M.J.D. Clift, F. Herzog M. Minghetti, B. Johnston, A. Petri-Fink, B. Rothen-Rutishauser, J. R. Soc. Interface 10 (2013) 20130396

[15] J.W. Costerton, P.S. Stewart, E.P. Greenberg, Science 284 (1999) 1318

[16] M.A. Radzig, V.A. Nadtochenko, O.A. Koksharova, J. Kiwi, V.A. Lipasova, I.A. Khmel, Colloids Surf. B 102 (2013) 300

[17] Z. Jia, M. Ben Amar, A. Astafiev, V. Nadtochenko, A.B. Evlyukhin, B.N. Chichkov, X. Duten, A. Kanaev, J. Phys. Chem. C 116 (2012) 17239

[18] R. Azouani, A. Soloviev, M. Benmami, K. Chhor, J.-F. Bocquet, A. Kanaev, J. Phys. Chem. C 111 (2007) 16243

[19] S. Pal, Y.K. Tak, J.M. Song, Appl. Environ. Microbiol. 73 (2007) 1712

[20] National Committee for Clinical Laboratory Standards, Methods for dilution antimicrobial susceptibility tests for bacteria that grow aerobically, 5th edition, Approved Standard M7-A4, NCCLS, Wayne, PA, 2000

[21] D.W. Jackson, K. Suzuki, L. Oakford, J.W. Simecka, M.E. Hart, T. Romeo, J. Bacteriol. 184 (2002) 290

[22] J. Zaitseva, V. Granik, A. Belik, O. Koksharova, I. Khmel, Res. Microbiol. 160 (2009) 353

[23] G.B. Zavilgelskii, V.Yu. Kotova, I.V. Manukhov, Chem. Phys. 31 (2012) 15 (in Russian)

[24] C. Levard, S. Mitra, T. Yang, A.D. Jew, A.R. Badireddy, G.V. Lowry, G.E. Brown, Environ. Sci. Technol. 47 (2013) 5738

[25] S. Chernousova, M. Epple, Angew. Chem. Int. Ed. 52 (2013) 1636